arXiv:2511.13649v5 [cs.CV] 3 Jul 2026

Distribution Matching Distillation Meets Reinforcement Learning

Dengyang Jiang[1,2,3] Dongyang Liu[6,2] Zanyi Wang[6] Qilong Wu[2] Liuzhuozheng Li[1]
Hengzhuang Li[1] Xin Jin[2] David Liu[6,2] Changsheng Lu[1] Zhen Li[2]
Bo Zhang[4] Mengmeng Wang[5] Steven Hoi[2] Peng Gao[2,3]✉ Harry Yang[1]✉

[1]HKUST [2]Alibaba Group [3]SIAT, CAS [4]Shanghai AI Lab [5]ZJUT [6]CUHK

Code: https://github.com/vvvvvjdy/dmdr

Figure 1. **Images generated by Z-Image-Turbo [66] distilled through Decoupled-DMD [34] and DMDR.** Demonstrating excellent generation quality, ultra-realistic, outstanding concept understanding, and remarkable text rendering.

Abstract

Distribution Matching Distillation (DMD) facilitates efficient inference by distilling multi-step diffusion models into few-step variants. Concurrently, Reinforcement Learning (RL) has emerged as a vital tool for aligning generative models with human preferences. While both represent critical post-training stages for large-scale diffusion models, existing studies typically treat them as independent, sequential processes, leaving a systematic framework for their unification largely unexplored. In this work, we demonstrate that jointly optimizing these two objectives yields mutual benefits: RL enables more preference-aware and controllable distillation rather than uniformly compressing the full data distribution, while DMD serves as an effective regularizer to mitigate reward hacking during RL training. Building on these insights, we propose DMDR, a unified framework that incorporates Reward-Tilted Distribution Matching optimization alongside two dynamic distillation training strategies in the initial stage, followed by the joint DMD and RL optimization in the second stage. Extensive experiments demonstrate that DMDR achieves state-of-the-art visual quality and prompt adherence among few-step generation methods, even surpassing the performance of its multi-step teacher model.

✉Corresponding authors

1. Introduction

Diffusion models pre-trained on large-scale datasets have achieved remarkable performance in visual generation tasks [11, 27, 49, 50, 66]. However, their sampling process typically requires numerous iterative denoising steps [21, 33, 64], each involving a full forward pass through a large neural network. This requirement makes high-resolution text-to-image synthesis computationally demanding. Furthermore, base models often fail to produce images that align closely with human preferences and aesthetic criteria [25, 45, 73].

To enhance practical utility, researchers typically employ two post-training stages. First, step-distillation [4, 40, 42, 52, 80, 81], which compresses the original model into a generator capable of few-step sampling (e.g., 4 steps) for efficient sampling. Among such methods, Distribution Matching Distillation (DMD) [81] is widely recognized for its effectiveness in large-scale scenarios [10, 15, 38, 80] and has been adopted in prominent industrial applications [28, 60, 66]. Second, reinforcement learning (RL) [3, 35, 36, 63, 67, 76, 79, 87] aligns the model with human preferences to improve aesthetic quality. Despite progress in both domains, most existing studies address these objectives in isolation. Early efforts to incorporate RL into the distillation process were largely confined to a two-stage paradigm [12, 41, 47, 52] (exploring how to conduct RL on an already distilled model). Consequently, there remains a critical gap in the field: *a systematic framework to explore the unification and potential synergy between these two "temporarily separated" stages*.

To bridge this gap, we propose DMDR, a unified framework that seamlessly integrates DMD and RL into a synergistic training pipeline. Our core insight is that concurrent optimization yields mutual benefits: (1) Preference-Aware Distillation: RL steers the distillation process toward high-reward regions, breaking the "performance ceiling" inherent in purely mimicking a teacher; (2) Distributional Regularization: The DMD objective serves as a robust regularizer for RL, mitigating reward hacking by maintaining proximity to the teacher's manifold. Specifically, DMDR operates in two stages. In the initial stage, we implement Reward-Tilted Distribution Matching (RT-DM), which distills toward a reward-tilted teacher distribution to prioritize human-preferred regions. Concurrently, we introduce Dynamic Distribution Guidance (DynaDG) and Dynamic Renoise Sampling (DynaRS) to stabilize the "cold-start" phase through annealed distributional overlap maximization. In the second stage, we transition to a joint optimization paradigm. In this phase, the RL objective drives aggressive preference alignment, while the DMD mechanism serves as a robust regularizer to prevent reward hacking.

Our experimental results show that our method leads to state-of-the-art few-step generative models. Moreover, our method is not only compatible with different models (e.g., flow-based, denoising-based) but also with various RL algorithms (e.g., ReFL, DPO, GRPO). This ensures the long-term effectiveness of our method as the multi-step model and RL algorithm evolve.

In summary, our main contributions are as follows:

- We propose DMDR, which shows that DMD and RL can be trained simultaneously with mutual benefits.
- We design a Reward-Tilted Distribution Matching and two dynamic distillation training strategies for better integrating RL and distillation in the initial phase.
- We validate our method on various models and RL algorithms, all of which achieve excellent performance.

2. Method

2.1. Preliminary

Distribution matching distillation. DMD [81] compresses a multi-step diffusion model (teacher) into a few-step generator (student) G by minimizing the time-averaged approximate Kullback-Leibler (KL) divergence between the real distribution $p_{\text{real},t}$ and the synthetic distribution $p_{\text{fake},t}$. Note that G is optimized via gradient descent, and this gradient admits a compact expression as the difference of two score functions:

$$\begin{aligned}\nabla_\theta \mathcal{L}_{\text{dmd}} &= \mathbb{E}_t[\nabla_\theta \operatorname{KL}(p_{\text{fake},t} \,\|\, p_{\text{real},t})] \\ &= \mathbb{E}_t\left[\nabla_\theta \mathbb{E}_{\boldsymbol{x}_0 \sim p_{\text{fake},t}}\left[\log \frac{p_{\text{fake},t}(\boldsymbol{x}_0)}{p_{\text{real},t}(\boldsymbol{x}_0)}\right]\right] \\ &= -\mathbb{E}_t\left[\int \Big(s_{\text{real}}(F_t) - s_{\text{fake}}(F_t)\Big) \frac{\mathrm{d}G_\theta(z)}{\mathrm{d}\theta}\, \mathrm{d}z\right],\end{aligned} \tag{1}$$

where $z \sim \mathcal{N}(0, \mathbf{I})$, θ denotes the parameters of G, and F_t is the forward diffusion operator that injects noise at time t to $G_\theta(z)$. The quantities s_{real} and s_{fake} are the score functions estimated by diffusion models μ_{real} and μ_{fake}, respectively. During training, the μ_{fake} is updated via diffusion loss $\mathcal{L}_{\text{diff}}$ (for denoising-based models, the prediction target is noise, while for flow-based ones, it is velocity) on synthetic samples produced by the few-step generator. Moreover, as introduced in DMD2 [80],

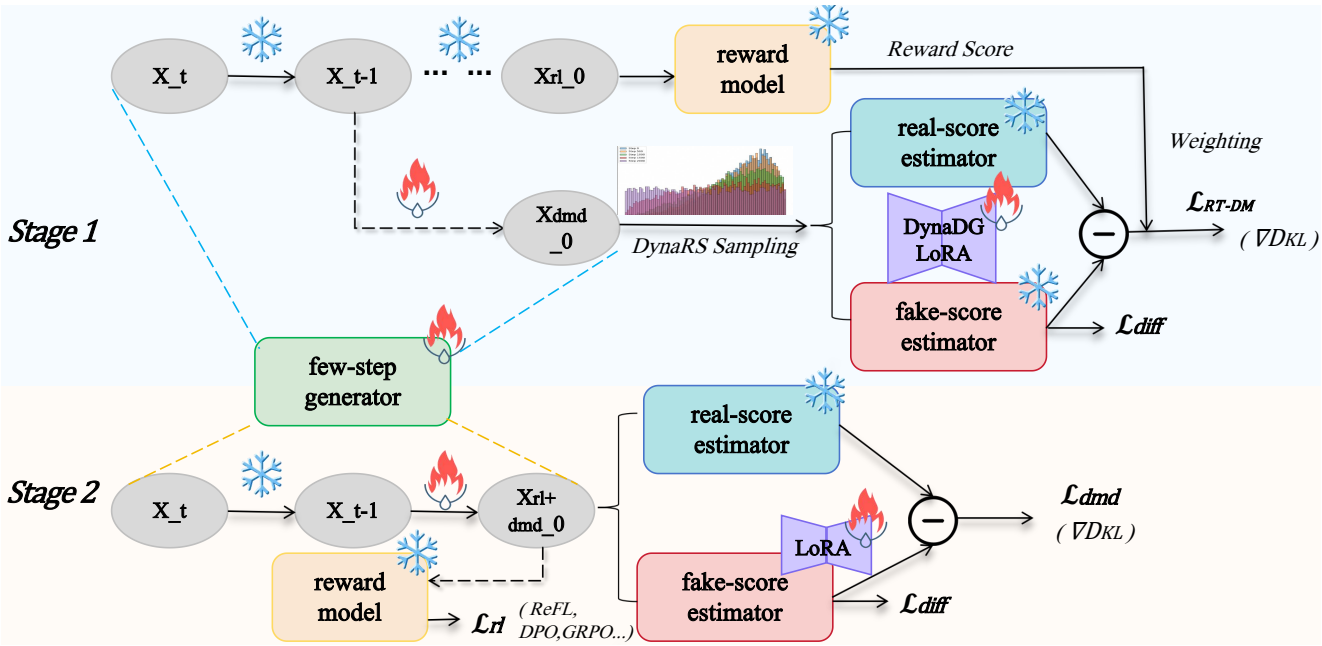

Figure 2. **Overview of DMDR**. It follows a two-stage training paradigm: Stage 1 (Reward-Tilted Distribution Matching) employs reward-weighted distillation to integrate preference signals into the early distillation phase, stabilized by Dynamic Distribution Guidance (DynaDG) and Dynamic Renoise Sampling (DynaRS). Stage 2 (Joint RL + DMD) performs direct reward maximization regularized by the DMD loss.

$G_\theta(z)$ is a noisy synthetic image produced by the current G running several steps, which is called backward simulation. The generator G then denoises these simulated images, and the outputs are supervised with the above loss functions.

Reinforce learning for diffusion models. Although there are various RL algorithms [35, 67, 76], All their goal is to optimize the diffusion model to generate the samples that can maximize a score given by reward models [19, 25, 73]. This score can be expressed as aesthetic, texture, prompt following, and so on. At the same time, a regularization term is often added to balance the trade-off between reward maximization and the deviation from the original model [89]. Thus, the loss can be formulated as follows:

$$\mathcal{L}_{\text{rl}} = \mathbb{E}\left[r(\boldsymbol{x}_0) - \text{KL}(p_{new} \| p_{\text{ref}})\right], \tag{2}$$

where r is the reward function, p_{new} and p_{ref} is the distribution of the trainable model and the reference (this can be a pre-train data distribution [76] or the original model's [35, 67, 87]), $\boldsymbol{x}_0$ is the clean image that is generated by the training generation model.

2.2. Problem Formulation and Pipeline Overview.

It is noted that DMD effectively reduces the sampling steps of the diffusion model, while RL enables the diffusion model to generate instruction-aligned and human-preferred images. Both of these are crucial for the practical application of the diffusion model. However, at present, the majority of the work [35, 38, 61, 79, 80, 87] only focuses on studying and improving one aspect, without exploring the synergy between the two. And only a small portion of the works [5, 12, 41, 47, 52] attempt to introduce RL into the distillation process, but they still focus on how to conduct RL on a distilled model. This raises a question: *Can these two be combined into one stage and benefit each other?*

We address this challenge question by proposing DMDR, as shown in Figure 2, the training process of DMDR is divided into two operational stages: Stage 1: RT-DM with Dynamic Distillation. (Section 2.4 and Section 2.5) Stage 2: Joint RL + DMD Optimization(Section 2.3). The following sections will provide the detailed analysis and illustration.

2.3. Bring DMD and RL Together with Benefit

We now show formally and empirically that DMD operates as a superior regularization mechanism that subsumes the traditional KL penalty in RL for few-step model, yielding robust joint optimization.

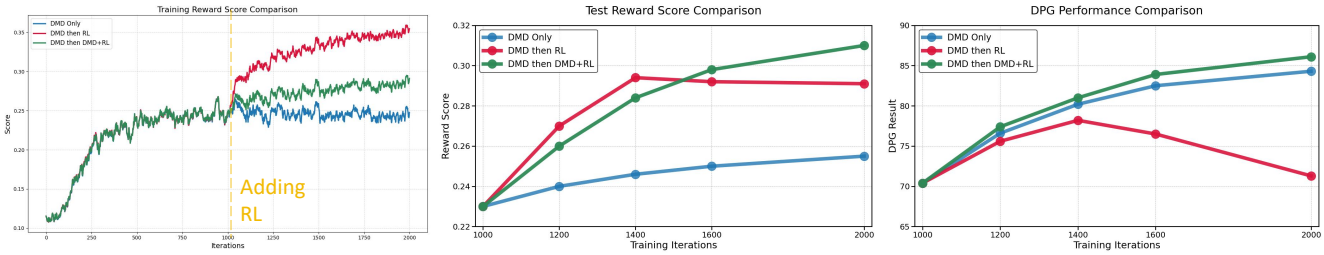

(a) Training Reward Score Comparison (b) Test-set Reward Score Comparison (c) DPG Score Comparison

Figure 4. **Verification of the joint optimization synergy.** Directly conduct RL (red) on the distilled model exhibits high training rewards but suffers from reward hacking and semantic collapse (low DPG score). In contrast, the joint DMD+RL paradigm (green) effectively boosts the performance (better than the DMD baseline (blue) in all metric) while preventing reward hacking. Better to zoom in to check the effect.

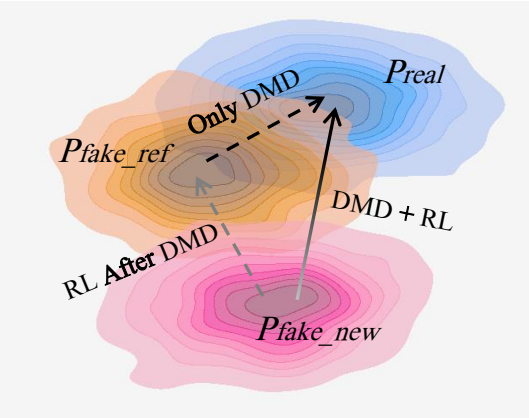

Figure 3. Visualization of the difference of optimization directions.

From the perspective of RL, standard preference optimization requires a penalty (e.g., $\mathrm{KL}(p_{new}\|p_{\text{ref}})$) to prevent reward hacking [35, 76]. In few-step models, sequentially applying RL after distillation uses the already-distilled distribution $P_{\text{fake-ref}}$ as the regularizer (Fig. 3). Because distillation inherently loses some modes, $P_{\text{fake-ref}}$ acts as an impoverished anchor, leading to rapid overfitting and mode collapse [52]. More fundamentally, instead of viewing DMD and RL as two disparate losses added heuristically, we reframe the joint objective as maximizing reward under a distribution-level structural constraint. As the joint gradient can be decomposed into two orthogonal objectives [59, 65, 89]: a "reward ascent" direction that increases human preference, and a "manifold projection" term that corrects off-manifold displacement by pulling the student back toward the teacher's regions.The DMD gradient $\nabla_\theta \mathcal{L}_{\text{dmd}}$ corresponds exactly to the maximum likelihood update projecting the student output distribution toward the learned data distribution of the multi-step teacher P_{real}. When combined linearly with the reward gradient $\nabla_\theta \mathcal{L}_{\text{rl}}$, any displacement induced by r that exits the teacher's high-density manifold generates a large discrepancy $s_{\text{real}} - s_{\text{fake}}$. The $\mathcal{L}_{\text{dmd}}$ gradient thus projects the reward ascent strictly along the teacher's support.

Simultaneously, from the perspective of distillation, pure DMD forces the student to uniformly mimic the teacher, implicitly establishing a "performance ceiling" capped by distilling P_{real} equally. Incorporating the RL objective addresses this fundamental limitation: RL steers the distillation toward high-reward regions, allowing the student to surpass the teacher while the DMD regularizer ensures semantic integrity is preserved.

Table 1. **Comparison of different training strategies.** The joint approach avoids the "distillation gap" of "RL then distillation" pipeline, achieving the highest preference score with $\sim 10\times$ rollout speedup.

Method	HPS	DPG	Time
SD3-M, resolution 1024×1024, local batchsize 16 on H100			
Multi-Step RL	31.06	86.43	9.24s $\sim$ 10.57s
Multi-Step RL then Distillation	30.42	85.92	-
Few-Step Joint RL and DMD	31.42	86.08	0.43s $\sim$ 1.21s

To validate the analysis, we conduct a comparative study using SD3-M [11] as the base model, with rewards provided by HPS v2.1 [73] and ReFL-based RL [76] for training. We compare three paradigms: (i) DMD Only (Blue line); (ii) DMD then RL (Sequential: distillation followed by RL in red line); and (iii) DMD then DMD+RL (Joint approach: distillation followed by joint optimization in green line). We evaluate these models across training/test reward curves and the DPG_Bench score [23]. As shown in Fig. 4(a), when RL is introduced (after 1000 iterations), the sequential approach achieves the highest training reward. However, this gain is obtained through hacking score. Fig. 4(b) and (c) reveal that this it suffers from severe reward hacking and catastrophic forgetting. While its training reward climbs, its test reward plateaus, and

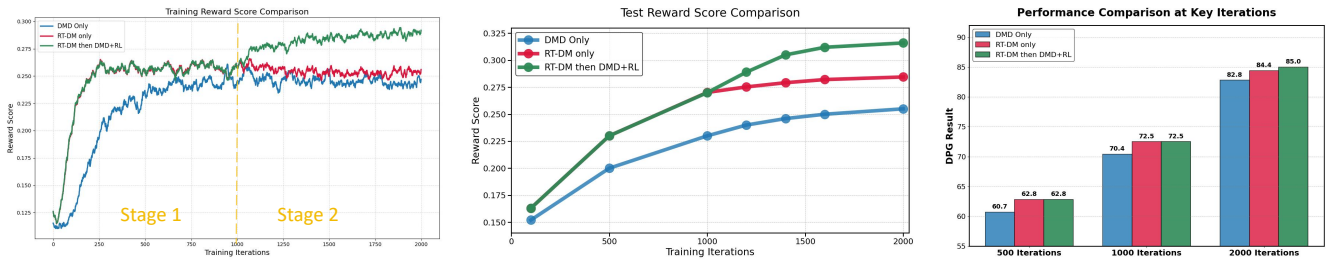

(a) Training Reward Score Comparison (b) Test-set Reward Score Comparison (c) DPG Score Comparison

Figure 5. **Effectiveness of RT-DM and two-stage training strategy.** In Stage 1, the RT-DM paradigm (red/green) significantly accelerates preference alignment compared to the DMD baseline (blue). In Stage 2, while "RT-DM only" (red) eventually saturates due to the constraints of the teacher's manifold, the transition to joint DMD+RL (green) successfully breaks this performance plateau by directly optimizing the reward score. This complete two-stage approach achieves the highest test rewards and DPG scores. Better to zoom in to check the effect.

its DPG score collapses. This confirms that without the strong distributional anchor of the teacher, the few-step model quickly drifts into narrow, high-reward modes that sacrifice semantic integrity [52]. In contrast, the joint optimization demonstrates a clear synergistic effect. First, it effectively breaks the "performance ceiling" of the teacher; the test reward significantly surpasses the DMD-only baseline. Second, by treating the DMD loss as a persistent structural regularizer, the model keeps improving DPG score while increasing aesthetic quality. This indicates that the DMD objective prevents the RL process from hacking, while the RL objective guides the distillation toward more human-preferred regions.

Based on the empirical synergy observed above, we formally define the optimization objective. The total loss is formulated as:

$$\mathcal{L}_{\text{total}} = \mathcal{L}_{\text{dmd}} + \lambda_{\text{rl}} \mathcal{L}_{\text{rl}}, \tag{3}$$

where $\mathcal{L}_{\text{dmd}}$ is the original distribution matching loss with the gradient formulated in Eq. 1, and $\mathcal{L}_{\text{rl}}$ is the plug-and-play reward maximization loss from the RL branch (Eq. 1), the gradient can be differentiable type like ReFL, or policy type like GRPO, etc. The hyperparameter λ_{rl} is a balancing coefficient used to trade off the two losses.

2.4. Reward-Tilted Distribution Matching for Integrating RL into the Early Phase of DMD

While we have demonstrated that DMD and RL can be trained jointly with mutual benefit, we still rely on a two-stage paradigm that incorporates RL only after an initial "cold start" distillation phase [41, 52]. This requirement stems from the observation that reward models typically necessitate a baseline generation capability to produce reliable feedback [63, 76]. Specifically, in DMD frameworks with flow matching model, the image used for gradient computation is defined as $\boldsymbol{x}_t - (0 - t)G_\theta(\boldsymbol{x}_t)$, where $\boldsymbol{x}_t$ is iteratively sampled. Notably, t can be any training time-step; thus, when training a 4-step model, the clean image can be generated in only one to four steps. In the early training phase, however, such few-step sampling often fails to produce coherent images, rendering reward signals noisy and unreliable for direct optimization.

To address this, we propose a Reward-Tilted Distribution Matching (RT-DM) paradigm to "softly" integrate reward signals into the distillation process. Specifically, we utilize the reward score as a weighting factor for the DMD loss. This formulation enables a more flexible optimization objective compared to direct reward maximization. This is because the reward score serves as a static weighting factor, we avoid the necessity of backpropagating through the multi-step denoising process, which allows us to evaluate the reward on the complete trajectory of the few-step model (e.g., 4 steps) without the computational overhead of a large gradient graph, bypassing the need for single-step $\boldsymbol{x}_0$ approximations to make the reward score more precise and highly valuable as a reference for optimization efforts. More profoundly, we are changing *which* distribution the student learns by assigning larger gradients to regions with higher reward scores, so that the model is not merely encouraged to match the real distribution defined by the teacher, but is instead biased toward better aligning with regions of the teacher distribution that yield higher reward scores. The gradient is formulated as:

$$\begin{aligned}
\nabla_\theta \mathcal{L}_{\text{RT-DM}} &= \mathbb{E}_t \Big[\nabla_\theta \Big(\mathrm{KL}(p_{\text{fake},t} \,\|\, p_{\text{real},t}) \; R(\boldsymbol{x}_0) \Big) \Big] \\
&= \mathbb{E}_t \left[\nabla_\theta \mathbb{E}_{\boldsymbol{x}_0 \sim p_{\text{fake},t}} \left[R(\boldsymbol{x}_0) \log \frac{p_{\text{fake},t}(\boldsymbol{x}_0)}{p_{\text{real},t}(\boldsymbol{x}_0)} \right] \right] \\
&= -\mathbb{E}_t \left[\int R(\boldsymbol{x}_0) \Big(s_{\text{real}}(F_t) - s_{\text{fake}}(F_t) \Big) \frac{\mathrm{d}G_\theta(z)}{\mathrm{d}\theta} \, \mathrm{d}z \right],
\end{aligned} \tag{4}$$

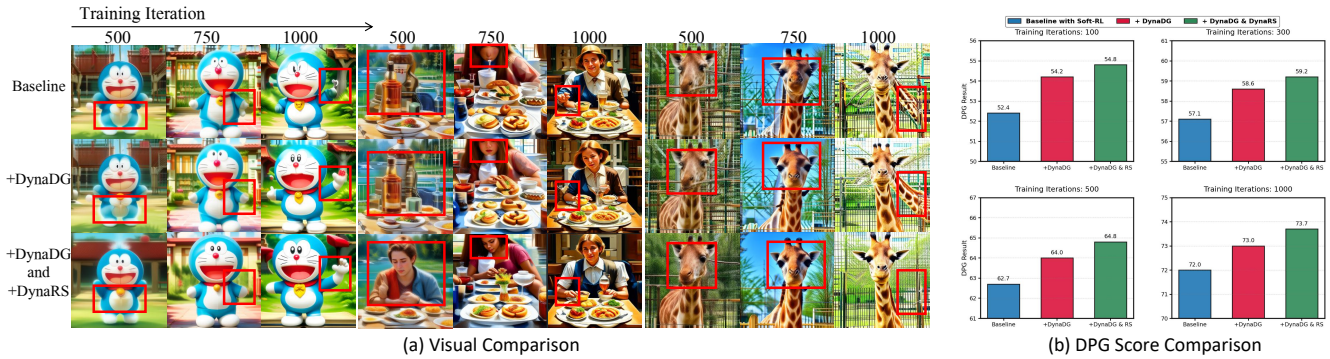

Figure 7. **Impact of dynamic training strategies**. (a) Qualitative comparisons show that our dynamic strategies facilitate faster global structure building (highlighted in red boxes). (b) Quantitative DPG scores further confirm that DynaDG and DynaRS provide more reliable optimization signals, consistently outperforming the baseline throughout Stage 1. Better to zoom in to check the effect.

where $R(\boldsymbol{x}_0) = e^{\frac{r(\boldsymbol{x}_0)}{\beta}}$, In our experiments, we set $\beta = \max_{\boldsymbol{x}'_0 \in \mathcal{B}} r(\boldsymbol{x}'_0)$, the maximum reward within the current mini-batch, to control the scale of the reward-induced weighting and prevent excessively large gradients.

To evaluate the effectiveness of the proposed soft integration, we compare three configurations in Fig. 5: (i) DMD Only (Blue); (ii) RT-DM for the entire duration (Red); and (iii) RT-DM followed by joint DMD+RL (Green). As shown in Fig. 5(a) and (b), the RT-DM paradigm (Red/Green) provides a significant "warm start" effect, accelerating preference alignment in the early phase (Stage 1) compared to the DMD-only baseline. This confirms that weighting the DMD loss with reward scores successfully incorporates preference signals even when few-step generations are still maturing, avoiding the noise instability of direct RL. However, the performance of the "RT-DM only" approach (Red) eventually saturates. We hypothesize that since RT-DM primarily acts by re-weighting the teacher's distribution gradients, its ability to drive the model toward high-reward regions is inherently constrained by the teacher's manifold. To further unlock the model's potential, we introduce a more direct reward maximization phase (Green) in Stage 2. By transitioning to joint DMD+RL optimization once the model has reached a stable baseline, we can leverage direct RL gradients to aggressively push the performance beyond the initial plateau. As a result, the joint approach achieves the highest test rewards and DPG scores, demonstrating that RT-DM serves as an ideal bridge to transition from pure distillation to direct preference alignment.

2.5. Annealed Distributional Overlap Maximization for Better Initial Distillation

During the initial phase of distillation, DMD encounters a classic "cold start" challenge: the synthetic samples generated by the few-step student exhibit substantial divergence from the real-world pre-training samples. This profound disjointness between P_{fake} and P_{real} impedes the teacher model's ability to estimate reliable scores, rendering the gradient $\nabla \log P_{\text{real}} - \nabla \log P_{\text{fake}}$ unreliable for optimization. To mitigate this, we introduce a unified principle of *annealed distributional overlap maximization*. We propose two complementary techniques to artificially increase the overlap between P_{fake} and P_{real} early in training, progressively relaxing them as the model converges.

Dynamic Distribution Guidance (DynaDG). DynaDG maximizes overlap primarily by actively shifting the target distribution. The poor initial Image quality causes P_{fake} to be disjoint from P_{real} (Figure 6, left). To solve this, we inject trainable LoRA modules [22] into the real score estimator to "pull" the perceived P_{real} toward the nascent P_{fake} (Figure 6, right). This ensures a reliable optimization signal by bridging the manifold gap. As training progresses, we anneal the LoRA scale in the teacher model toward zero, allowing the real score estimator to seamlessly revert to the true P_{real} once P_{fake} is safely anchored.

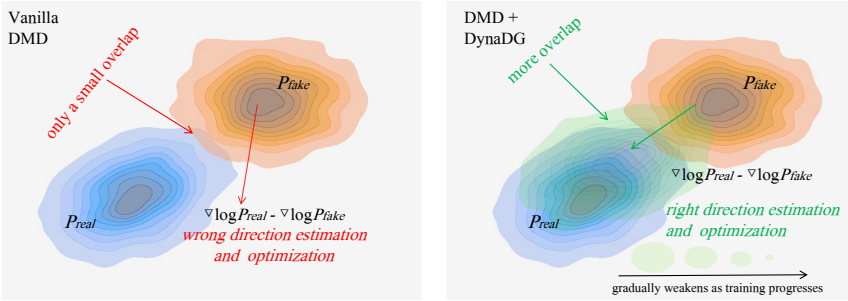

Figure 6. Illustration for Dynamic Distribution Guidance.

Dynamic Renoise Sampling (DynaRS). While DynaDG moves the distributions, DynaRS maximizes overlap by exploiting

Table 2. **System-level comparison** against state-of-the-art methods. ⋆ denotes our reproduced results based on the official code. Best performance is marked in **Bold**.

Method	NFE	Post-Train	CLIP Score↑	Aesthetic Score↑	Pick Score↑	HP Score↑
SDXL-Base						
Base-Model	50	-	34.7588	5.6480	22.1085	27.1477
ReFL [76]⋆	50	RL	35.2107	5.9045	22.8076	**33.1874**
LCM [40]	2	Distill	28.4664	5.1026	20.0603	17.6837
Lightning [30]	1	Distill	32.0283	5.6761	21.4868	26.3615
DMD2 [80]	1	Distill	34.3046	5.6238	21.7293	26.5986
DMDR (ours)	1	Distill & RL	**35.6241**	**6.1184**	**22.8498**	32.0065
DMD2 [80]	4	Distill	34.5169	5.7043	22.1546	28.5655
DMD2-PSO [47]⋆	4	Distill then RL	34.0128	5.8032	22.2644	29.8732
DMDR (ours)	4	Distill & RL	**35.4940**	**6.0324**	**22.7122**	32.9832
SD3-Medium						
Base-Model	50	-	34.9025	5.5942	22.1801	28.4021
ReFL [76]⋆	50	RL	**35.1851**	5.7821	22.0064	32.0745
DMD2 [80]⋆	4	Distill	33.9421	5.6137	21.7688	27.3675
Flash [4]	4	Distill	34.2634	5.6702	21.5921	26.6542
TDM [43]	4	Distill	34.0301	5.6250	22.0010	27.7522
Hyper-SD [52]	8	Distill then RL	32.0234	5.2489	20.2831	22.4544
DMDR (ours)	4	Distill & RL	35.0142	**5.8876**	**22.4892**	**32.1145**
SD3.5-Large						
Base-Model	50	-	35.5509	5.7014	22.4856	28.8135
LADD [56]	4	Distill then RL	35.0480	5.4514	22.2451	27.8470
DMDR (ours)	4	Distill & RL	**35.9757**	**6.1541**	**22.9072**	**32.7368**

regions where distributions naturally intersect. By heavily biasing the sampling of renoise levels t toward higher noise values at the start of training, we ensure that both initial samples and reference samples are dominated by Gaussian noise, placing them in a similar regime. At these high noise levels, the score estimator provides highly reliable gradients that emphasize global structure [85, 86]. As the student generator improves, the renoise bias is progressively annealed to uniform sampling, allowing the model to capture fine-grained textural details from a wider range of noise levels.

As shown in Figure 7 (b), our dynamic training strategies significantly enhance the initial training phase. Qualitative results presented in Figure 7 left further corroborate these findings, showing a faster global structure building when DynaDG and DynaRS are employed.

3. Experiments

3.1. Experimental Setup

For training, we adopt denoising-based model (SDXL-Base [50]) and flow-based models (SD3-Medium [11], SD3.5-Large [1]) for distillation, using prompts from t2i-2M. Additionally, we use ReFL [76] with DFN-CLIP [13] and HPSv2.1 [73] as reward models by default. As for evaluation, we validate the effect of DMDR through extensive experiments. First, we use prompts sampled from a recent public dataset ShareGPT-4o-Image [7] to generate images and follow previous work [38, 43] that report CLIP Score [19], Aesthetic Score [58], Pick Score [25], and Human Preference (HP) Score [73]. Next, in order to obtain a more comprehensive evaluation, we also compare our distilled models with their teachers on two popular benchmarks, DPG_Bench [23] and GenEval [16]. Noted that there are some differences from the settings we made in the Method section. We train 1.5K steps in stage1 and stage 2, respectively, to achieve better performance.

Method for comparison. We compare our method against several categories of existing work, including foundational multi-step base models [1, 11, 50], RL only approaches [76], distillation only methods [4, 30, 40, 43, 80], distillation then RL

Table 3. **GenEval Comparison:** 4-step (ours) $vs.$ its multi-step teacher.

Model	Overall	Single	Two	Count.	Colors	Pos.	Attr.
SDXL-Base							
Teacher	0.55	0.98	0.74	0.39	0.85	0.15	0.23
Ours	**0.57**	**0.99**	**0.76**	**0.44**	**0.85**	0.12	**0.25**
SD3-Medium							
Teacher	0.62	0.98	0.74	0.63	0.67	0.34	0.36
Ours	**0.65**	**0.99**	**0.84**	0.57	**0.81**	0.27	**0.45**
SD3.5-Large							
Teacher	0.71	0.98	0.89	0.73	0.83	0.34	0.47
Ours	**0.72**	**0.99**	**0.93**	0.69	0.80	0.31	**0.59**

Table 4. **DPG_Bench Comparison:** 4-step (ours) $vs.$ its multi-step teacher.

Model	Overall	Global	Entity	Attribute	Relation	Other
SDXL-Base						
Teacher	74.65	83.27	82.43	80.91	86.76	80.41
Ours	**76.48**	**83.72**	**82.58**	**83.69**	84.76	**83.54**
SD3-Medium						
Teacher	84.08	87.90	91.01	88.83	80.70	88.68
Ours	**85.30**	**90.49**	90.07	**90.56**	**87.17**	**91.23**
SD3.5-Large						
Teacher	84.12	91.48	90.22	87.81	91.20	89.49
Ours	**85.33**	90.47	**90.53**	**90.68**	87.44	**90.20**

Figure 8. Visual comparison between the teachers, selected competing methods [52, 56, 80], and ours. All images are generated using identical noise. Our model produces images with superior quality and prompt coherence.

frameworks [47, 52]. We do not compare with methods like Flash-DMD [5] and Diff-Instruct++ [41] that do not provide model weights or open source training code because we cannot guarantee a fair and reproducible evaluation.

3.2. Main Results

We begin by assessing DMDR's text-to-image generation performance using prompts sampled from ShareGPT-4o-Image [7], ensuring that there is no overlap with the prompts utilized during training. Table 2 presents a summary of the distillation results in comparison to other methods. Models distilled through our approach exhibit state-of-the-art (SOTA) capabilities in terms of prompt coherence and the generation of high-quality, aesthetically pleasing images. Notably, our method demonstrates effectiveness across various architectures (e.g., UNet, Transformer), model sizes (e.g., 2B, 8B), and paradigms (e.g., flow-based, denoising-based), highlighting the broad applicability and universality of the proposed approach. Additionally, we provide qualitative comparisons in Figure 8, where our method produces images characterized by superior quality and enhanced prompt coherence.

To further verify our method's effectiveness and provide a more comprehensive comparison between the few-step distillation model and the multi-step teacher model, we conduct the comparison on two commonly used benchmarks [16, 23], Although we do not perform RL optimization on the metric of these two benchmarks, table 4 and 3 show that the overall score of our four-step model consistently outperforms its multi-step teacher on DPG_Bench and GenEvalacross all base models. These results indicate that DMDR has successfully freed the student model from the constraints of the multi-step teacher model and stimulated its capabilities during the distillation process.

Table 5. Ablation on different components. Default settings are marked in purple.

(a) Ablation on different reward models.

Method	CLIP Score	Aesthetic Score	Pick Score	HP Score	DPG overall
Pick [25]	34.3403	5.9021	22.9674	31.7665	84.86
AE [58]	34.1748	6.1024	22.3858	31.6620	84.61
CLIP [19]	35.2087	5.5832	22.0644	28.0507	85.10
HPS [73]	34.4088	5.9021	22.5108	32.9065	85.04
CLIP + HPS	35.0142	5.8876	22.4892	32.1145	85.30

(b) Ablation on RL algorithm in stage 2.

Method	CLIP Score	Aesthetic Score	Pick Score	HP Score	DPG overall
stage 1 init	*33.3648*	*5.5744*	*21.0070*	*28.8371*	*82.4371*
w/ RL (ReFL)	35.0142	5.8876	22.4892	32.1145	85.30
w/ RL (DPO)	34.0234	5.8340	21.9844	30.8352	85.00
w/ RL (GRPO)	34.6675	5.9324	22.3248	31.4474	85.08

(c) Ablation on Value of λ_{rl}.

Value	CLIP Score	Aesthetic Score	Pick Score	HP Score	DPG overall
0.1	34.7422	5.8508	22.3064	31.6565	85.24
0.5	35.0142	5.8876	22.4892	32.1145	85.30
1.0	35.0087	5.84430	22.4709	32.8982	85.04
2.0	35.0322	5.7806	22.1098	32.7683	82.48

3.3. Ablation Study

In this section, we conduct a systematic investigation into the key components of DMDR. Unless otherwise specified, all experiments use the SD3-M base model with a 4-step sampling configuration.

Versatility across reward models. A key advantage of ourusing a DINOv2-based reward model to maximize classification accuracyDMDR is the ability to steer the distillation process toward diverse human preferences. As shown in Table 5a, we evaluate the framework using different reward models (RMs) targeting specific attributes. The results provide a clear insight: optimizing with a specific RM leads to a significant performance gain in its corresponding metric, confirming that DMDR effectively injects the desired preference signal into the few-step manifold. Furthermore, by integrating multiple rewards (CLIP + HPS), the model achieves a more balanced and superior generative performance, similar to the findings in DanceGRPO [79]. This flexibility allows users to customize the distillation "flavor" according to specific downstream tasks.

Compatibility with RL paradigms. To verify the algorithmic universality of our unified framework, we compare three distinct RL strategies in the Stage 2 joint optimization phase: ReFL [76], DPO [47, 67], and GRPO [35, 79]. As shown in Table 5b, all three algorithms yield substantial improvements over the "Stage 1 init" baseline across all evaluation dimensions. Furthermore, an interesting observation is that using the ReFL in DMDR achieves overall better performance, and our analysis is that: traditional ReFL for multi-step models ignores earlier sampling steps and only trains the last few steps before the output image [76] because the large computational graph generated by the multi-step denoising process would result in a huge memory consumption. Subsequent solutions [63, 75] mainly focus on saving forward noise trajectory and sampling a subset of steps to optimize, although this can allow the gradient to return to the early denoising step, it is also prone to error accumulation. On the contrary, in our few-step model, the model is trained to predict a clean image at each step's state [80], which enables the gradient of ReFL to directly return to the initial state, thus obtaining an effective optimization.

The balancing Role of DMD Regularization. The synergy between distillation and RL is governed by the balancing coefficient λ_{rl} in our joint objective. Table 5c illustrates the trade-off between reward maximization and distributional stability. When λ_{rl} is set too low; the model remains constrained by the teacher's manifold, limiting the potential for preference alignment. Conversely, as it increases beyond an optimal threshold, we observe a noticeable decline in a general capacity (reflected by the DPG overall score), despite high reward scores. This trend provides a crucial insight: the DMD loss serves as a vital structural regularizer. It prevents the model from "reward hacking"(We also showed in Figure 4. The optimal balance ensures that the model pushes the boundaries of quality while staying anchored to the teacher's robust generative priors.

4. Limitation and Discussion

Quality vs. Diversity. To further analyze the behavior of DMDR, we conduct class-conditional experiments on ImageNet 256×256 using the SiT [24, 44, 82] backbone for 1-step generation and text-to-image settings used in the former paper. As shown in Table 6, a fundamental trade-off between generative quality and diversity emerges. Our results reveal that both Classifier-Free Guidance (CFG) (this also observed in Decoupled-DMD [34]) and Reinforcement Learning (here we use a DINOv2-based [48] reward model to maximize classification accuracy) act as "density sharpeners" during distillation.

Table 6. **1-step SiT DMDR Results on ImageNet** 256×256. We report the performance with different CFG scales and RL optimization. Metrics include FID [20], Recall [26], Inception Score (IS) [55], and Precision [26].

CFG	RL	FID ↓	Recall ↑	Inception Score ↑	Precision ↑
No	No	2.13	0.64	232.15	0.77
1.5	No	5.20	0.48	387.24	0.88
4	No	15.70	0.11	453.65	0.86
No	Yes	6.95	0.40	416.01	0.90
1.5	Yes	13.43	0.24	494.43	0.93

Table 7. Diversity evaluation on ShareGPT-4o-Image [7].

Metric	Base-Model	DMD	DMD2	Base + ReFL	DMD + PSO	DMDR
HPS↑	28.4021	28.0248	27.3675	32.0745	30.1180	32.1145
LPIPS↑	0.6840	0.5664	0.5832	0.5602	0.5540	0.5548

Table 8. Impact of the trade-off λ_{rl}.

Metric	Base-Model	DMD	DMDR $\lambda_{\text{rl}}0.1$	DMDR $\lambda_{\text{rl}}0.5$	DMDR $\lambda_{\text{rl}}1$
HPS↑	28.4021	28.0248	30.4024	32.1145	32.4786
LPIPS↑	0.6840	0.5664	0.5602	0.5548	0.5266

We believe this reduction in diversity is not a limitation unique to our approach, but a characteristic of score-based distillation and preference alignment, which steer the model toward high-reward, high-confidence regions. We also provide additional experiments with LPIPS diversity [84] on SD3-medium in Table 7, which shows similar degradation as on ImageNet and for other methods, while DMDR provides a favorable quality/alignment trade-off. Although DMD regularization mitigates reward hacking compared with direct/sequential RL (shown in Figure 4), it cannot completely remove the inherent diversity cost of reward optimization. This trade-off is tunable: a smaller λ_{rl} improves diversity with reduced preference gains as shown in Table 8, allowing users to balance the trade-off. More explorations on adaptive reward weighting and other diversity-preserving RL objectives could be future work.

5. Related Work

Distribution matching distillation. Distribution Matching Distillation [81] (DMD) is the first work to successfully apply the principle score-based distillation [51, 65, 70] to large-scale text-to-image models. Intuitively, it strives to ensure that any sample realized by the student at a given noise level occurs with exactly the same probability as it would under the teacher's distribution, thereby preserving the multi-step generative priors in the few-step model. From then on, a lot of follow-up work emerged [2, 5, 10, 38, 43, 78, 80], for example, DMD2 [80] employs a discriminator to align the student model distribution with a specific target distribution like GAN [17] does; TDM [43] incorporates DMD loss in the sampling process of the student model for better alignment; f–distill [78] replaces the original reverse Kullback–Leibler (KL) divergence to the proposed f-divergence for covering different divergences with different properties. Our work also starts with DMD, but we don't focus on how to better "imitate" the teacher. Instead, we aim to incorporate reinforcement learning in the distillation process to enable a more controllable and preference-aligned distillation.

Reinforce learning for diffusion models. Reinforce learning helps to align diffusion models to human preferences by training a reward model and using it to guide generation [3, 35, 63, 67, 76, 79, 87]. There are many algorithms to conduct RL, for example, DDPO [3] adapts PPO via image log-likelihoods; ReFL [76] bypasses likelihoods by optimizing outputs with frozen-reward gradients; Diffusion-DPO [67] adapts DPO to diffusion for paired human preference data; and recent GRPO extensions [35, 79] use GRPO to diffusion models by coupling the training loss with SDE samplers. Although significant progress has been made in RL for diffusion models, most of the work has focused on multi-step models. Here, we find that these algorithms are also adapted to the few-step model when carried out in conjunction with distribution matching distillation.

Trajectory-based distillation. Trajectory-based distillation [6, 40, 52, 88], which typically aims to simulate teacher ODE

trajectories on the instance level. Early work [39] regresses the teacher's ODE integral in one step, producing blurry ℓ_2–x_0 estimates, and thus suffers from degraded quality. Progressive distillation [14, 52] mitigates this by a multi-stage pipeline that enlarges the student's step size and halves its NFE each stage by distilling the prior stage's trajectory into fewer steps, However, this not only makes the training a multi-stage process (e.g., NFE from 50 to 25 then to 10, etc.), but also leads to cumulative errors. Meanwhile, consistency models [37, 40] aim to learn a consistency function that maps the point at an arbitrary time t on the teacher's PF-ODE trajectory to the initial point. However, the student model must be constructed implicitly using either inaccurate finite differences or expensive Jacobian–vector products (JVPs) and the quality is still limited due to the accumulation of errors into the integrated state, which limits the application in large-scale scenarios [6, 88].

Adversarial distillation. Adversarial distillation [31, 32, 56, 57] can be regarded as another form of distribution matching distillation. The difference is that adversarial distillation aim to estimate the distribution of both the student model and the real data or the teacher model through a discriminator model [17] to match the distribution. Representative works like Adversarial Diffusion Distillation (ADD) [57] force the few-step student diffusion model to fool a discriminator which is trained to distinguish the generated samples from real images. Follow-up works [31, 32] applied this idea to other fields. However, such a training method can cause many instabilities, similar to traditional GANs [17, 54], hence requires a lot of tricks to stabilize training [29, 46, 53].

Other distillation works. Other distillation works mainly focus on combining the distillation at the distribution level and the trajectory level [8, 9, 43, 88]. For example, SANA-Sprint [8] combines the ideas of LADD [56] and sCM [37] and achieves fast convergence and high fidelity generation while retaining the alignment advantages of sCMs. TDM [43] and rCM [88] combine DMD [81] and LCM [40] together to remedy the quality issues of LCM.

Reward models for diffusion post-train. Unlike Large Language Models (LLMs), where reinforcement learning (RL) can often leverage verifiable, rule-based rewards [18, 62, 83] (e.g., code execution success or mathematical correctness), diffusion-based image generation is inherently subjective. The evaluation of generated images relies heavily on multifaceted criteria such as aesthetic quality, instruction following, and so on, which are difficult to quantify through rigid, rule-based functions. Consequently, the development of robust reward models (RMs) has become a critical prerequisite for effective RL-based alignment in diffusion models [19, 71, 72, 74, 76, 77]. Early methods, such as CLIP-score [19], primarily focus on measuring the semantic alignment between the text prompt and the generated image. To address the need for visual fidelity and artistic appeal, metrics like Aesthetic Score [58] and HPS (Human Preference Score) [45, 73, 74] have been introduced to capture the nuance of human aesthetic judgment. More recently, the reward models become unified [68, 69, 77] and aggregate multi-dimensional preferences—ranging from low-level texture details to high-level semantic instruction following—into a unified scoring function. While our primary contribution lies in proposing a novel algorithm that integrates few-step distillation with reinforcement learning, our empirical results highlight the pivotal role of the reward model in our pipeline.

6. Conclusion

We introduces DMDR, a unified framework that transforms Distribution Matching Distillation (DMD) and Reinforcement Learning (RL) from independent, sequential stages into a synergistic training pipeline. We demonstrate that joint optimization is mutually beneficial: RL steers distillation toward high-reward regions to break the "teacher ceiling," while DMD regularizes RL to effectively mitigate reward hacking. By employing a two-stage strategy—incorporating RT-DM and dynamic training followed by joint optimization—DMDR achieves state-of-the-art few-step performance across diverse architectures. Ultimately, our approach enables few-step models to not only match but consistently surpass the visual quality and prompt adherence of their original multi-step teacher models.

References

[1] Stability AI. Sd3.5. https://github.com/Stability-AI/sd3.5, 2024. 7

[2] Hmrishav Bandyopadhyay, Rahim Entezari, Jim Scott, Reshinth Adithyan, Yi-Zhe Song, and Varun Jampani. Sd3. 5-flash: Distribution-guided distillation of generative flows. *arXiv preprint arXiv:2509.21318*, 2025. 10

[3] Kevin Black, Michael Janner, Yilun Du, Ilya Kostrikov, and Sergey Levine. Training diffusion models with reinforcement learning. *arXiv preprint arXiv:2305.13301*, 2023. 2, 10

[4] Clement Chadebec, Onur Tasar, Eyal Benaroche, and Benjamin Aubin. Flash diffusion: Accelerating any conditional diffusion model for few steps image generation. In *Proceedings of the AAAI Conference on Artificial Intelligence*, pages 15686–15695, 2025. 2, 7

[5] Guanjie Chen, Shirui Huang, Kai Liu, Jian-Xiang Zhu, Xiaoye Qu, Peng Chen, Yu Cheng, and Yifu Sun. Flash-dmd: Towards high-fidelity few-step image generation with efficient distillation and joint reinforcement learning. *ArXiv*, abs/2511.20549, 2025. 3, 8, 10

[6] Hansheng Chen, Kai Zhang, Hao Tan, Leonidas Guibas, Gordon Wetzstein, and Sai Bi. pi-flow: Policy-based few-step generation via imitation distillation. *arXiv preprint arXiv:2510.14974*, 2025. 10, 11

[7] Junying Chen, Zhenyang Cai, Pengcheng Chen, Shunian Chen, Ke Ji, Xidong Wang, Yunjin Yang, and Benyou Wang. Sharegpt-4o-image: Aligning multimodal models with gpt-4o-level image generation. *arXiv preprint arXiv:2506.18095*, 2025. 7, 8, 10

[8] Junsong Chen, Shuchen Xue, Yuyang Zhao, Jincheng Yu, Sayak Paul, Junyu Chen, Han Cai, Song Han, and Enze Xie. Sana-sprint: One-step diffusion with continuous-time consistency distillation. *arXiv preprint arXiv:2503.09641*, 2025. 11

[9] Jiaxiang Cheng, Bing Ma, Xuhua Ren, Hongyi Jin, Kai Yu, Peng Zhang, Wenyue Li, Yuan Zhou, Tianxiang Zheng, and Qinglin Lu. Pose: Phased one-step adversarial equilibrium for video diffusion models. *arXiv preprint arXiv:2508.21019*, 2025. 11

[10] Zhenglin Cheng, Peng Sun, Jianguo Li, and Tao Lin. Twinflow: Realizing one-step generation on large models with self-adversarial flows. *arXiv preprint arXiv:2512.05150*, 2025. 2, 10

[11] Patrick Esser, Sumith Kulal, Andreas Blattmann, Rahim Entezari, Jonas Müller, Harry Saini, Yam Levi, Dominik Lorenz, Axel Sauer, Frederic Boesel, et al. Scaling rectified flow transformers for high-resolution image synthesis. In *Forty-first international conference on machine learning*, 2024. 2, 4, 7

[12] Luca Eyring, Shyamgopal Karthik, Alexey Dosovitskiy, Nataniel Ruiz, and Zeynep Akata. Noise hypernetworks: Amortizing test-time compute in diffusion models. *arXiv preprint arXiv:2508.09968*, 2025. 2, 3

[13] Alex Fang, Albin Madappally Jose, Amit Jain, Ludwig Schmidt, Alexander Toshev, and Vaishaal Shankar. Data filtering networks. *arXiv preprint arXiv:2309.17425*, 2023. 7

[14] Kevin Frans, Danijar Hafner, Sergey Levine, and Pieter Abbeel. One step diffusion via shortcut models. *arXiv preprint arXiv:2410.12557*, 2024. 11

[15] Xingtong Ge, Xin Zhang, Tongda Xu, Yi Zhang, Xinjie Zhang, Yan Wang, and Jun Zhang. Senseflow: Scaling distribution matching for flow-based text-to-image distillation. *arXiv preprint arXiv:2506.00523*, 2025. 2

[16] Dhruba Ghosh, Hannaneh Hajishirzi, and Ludwig Schmidt. Geneval: An object-focused framework for evaluating text-to-image alignment. *Advances in Neural Information Processing Systems*, 36:52132–52152, 2023. 7, 8

[17] Ian Goodfellow, Jean Pouget-Abadie, Mehdi Mirza, Bing Xu, David Warde-Farley, Sherjil Ozair, Aaron Courville, and Yoshua Bengio. Generative adversarial nets. *Advances in neural information processing systems*, 27, 2014. 10, 11

[18] Daya Guo, Dejian Yang, Haowei Zhang, Junxiao Song, Peiyi Wang, Qihao Zhu, Runxin Xu, Ruoyu Zhang, Shirong Ma, Xiao Bi, et al. Deepseek-r1: Incentivizing reasoning capability in llms via reinforcement learning. *arXiv preprint arXiv:2501.12948*, 2025. 11

[19] Jack Hessel, Ari Holtzman, Maxwell Forbes, Ronan Le Bras, and Yejin Choi. Clipscore: A reference-free evaluation metric for image captioning. *arXiv preprint arXiv:2104.08718*, 2021. 3, 7, 9, 11

[20] Martin Heusel, Hubert Ramsauer, Thomas Unterthiner, Bernhard Nessler, and Sepp Hochreiter. Gans trained by a two time-scale update rule converge to a local nash equilibrium. *Advances in neural information processing systems*, 30, 2017. 10

[21] Jonathan Ho, Ajay Jain, and Pieter Abbeel. Denoising diffusion probabilistic models. *Advances in neural information processing systems*, 33:6840–6851, 2020. 2

[22] Edward J Hu, Yelong Shen, Phillip Wallis, Zeyuan Allen-Zhu, Yuanzhi Li, Shean Wang, Lu Wang, Weizhu Chen, et al. Lora: Low-rank adaptation of large language models. *ICLR*, 1(2):3, 2022. 6

[23] Xiwei Hu, Rui Wang, Yixiao Fang, Bin Fu, Pei Cheng, and Gang Yu. Ella: Equip diffusion models with llm for enhanced semantic alignment. *arXiv preprint arXiv:2403.05135*, 2024. 4, 7, 8

[24] Dengyang Jiang, Mengmeng Wang, Liuzhuozheng Li, Lei Zhang, Haoyu Wang, Wei Wei, Guang Dai, Yanning Zhang, and Jingdong Wang. No other representation component is needed: Diffusion transformers can provide representation guidance by themselves. *arXiv preprint arXiv:2505.02831*, 2025. 9

[25] Yuval Kirstain, Adam Polyak, Uriel Singer, Shahbuland Matiana, Joe Penna, and Omer Levy. Pick-a-pic: An open dataset of user preferences for text-to-image generation. *Advances in neural information processing systems*, 36:36652–36663, 2023. 2, 3, 7, 9

[26] Tuomas Kynkäänniemi, Tero Karras, Samuli Laine, Jaakko Lehtinen, and Timo Aila. Improved precision and recall metric for assessing generative models. *Advances in neural information processing systems*, 32, 2019. 10

[27] Black Forest Labs. Flux. https://github.com/black-forest-labs/flux, 2024. 2

[28] Black Forest Labs. FLUX.2: Frontier Visual Intelligence. https://bfl.ai/blog/flux-2, 2025. 2

[29] Shanchuan Lin and Xiao Yang. Animatediff-lightning: Cross-model diffusion distillation. *arXiv preprint arXiv:2403.12706*, 2024. 11

[30] Shanchuan Lin, Anran Wang, and Xiao Yang. Sdxl-lightning: Progressive adversarial diffusion distillation. *arXiv preprint arXiv:2402.13929*, 2024. 7

[31] Shanchuan Lin, Xin Xia, Yuxi Ren, Ceyuan Yang, Xuefeng Xiao, and Lu Jiang. Diffusion adversarial post-training for one-step video generation. *arXiv preprint arXiv:2501.08316*, 2025. 11

[32] Shanchuan Lin, Ceyuan Yang, Hao He, Jianwen Jiang, Yuxi Ren, Xin Xia, Yang Zhao, Xuefeng Xiao, and Lu Jiang. Autoregressive adversarial post-training for real-time interactive video generation. *arXiv preprint arXiv:2506.09350*, 2025. 11

[33] Yaron Lipman, Ricky TQ Chen, Heli Ben-Hamu, Maximilian Nickel, and Matt Le. Flow matching for generative modeling. *arXiv preprint arXiv:2210.02747*, 2022. 2

[34] Dongyang Liu, Peng Gao, David Liu, Ruoyi Du, Zhen Li, Qilong Wu, Xin Jin, Sihan Cao, Shifeng Zhang, Hongsheng Li, et al. Decoupled dmd: Cfg augmentation as the spear, distribution matching as the shield. *arXiv preprint arXiv:2511.22677*, 2025. 1, 9

[35] Jie Liu, Gongye Liu, Jiajun Liang, Yangguang Li, Jiaheng Liu, Xintao Wang, Pengfei Wan, Di Zhang, and Wanli Ouyang. Flow-grpo: Training flow matching models via online rl. *arXiv preprint arXiv:2505.05470*, 2025. 2, 3, 4, 9, 10

[36] Jie Liu, Gongye Liu, Jiajun Liang, Ziyang Yuan, Xiaokun Liu, Mingwu Zheng, Xiele Wu, Qiulin Wang, Wenyu Qin, Menghan Xia, et al. Improving video generation with human feedback. *arXiv preprint arXiv:2501.13918*, 2025. 2

[37] Cheng Lu and Yang Song. Simplifying, stabilizing and scaling continuous-time consistency models. *arXiv preprint arXiv:2410.11081*, 2024. 11

[38] Yanzuo Lu, Yuxi Ren, Xin Xia, Shanchuan Lin, Xing Wang, Xuefeng Xiao, Andy J Ma, Xiaohua Xie, and Jian-Huang Lai. Adversarial distribution matching for diffusion distillation towards efficient image and video synthesis. *arXiv preprint arXiv:2507.18569*, 2025. 2, 3, 7, 10

[39] Eric Luhman and Troy Luhman. Knowledge distillation in iterative generative models for improved sampling speed. *arXiv preprint arXiv:2101.02388*, 2021. 11

[40] Simian Luo, Yiqin Tan, Longbo Huang, Jian Li, and Hang Zhao. Latent consistency models: Synthesizing high-resolution images with few-step inference. *arXiv preprint arXiv:2310.04378*, 2023. 2, 7, 10, 11

[41] Weijian Luo. Diff-instruct++: Training one-step text-to-image generator model to align with human preferences. *arXiv preprint arXiv:2410.18881*, 2024. 2, 3, 5, 8

[42] Weijian Luo, Tianyang Hu, Shifeng Zhang, Jiacheng Sun, Zhenguo Li, and Zhihua Zhang. Diff-instruct: A universal approach for transferring knowledge from pre-trained diffusion models. *Advances in Neural Information Processing Systems*, 36:76525–76546, 2023. 2

[43] Yihong Luo, Tianyang Hu, Jiacheng Sun, Yujun Cai, and Jing Tang. Learning few-step diffusion models by trajectory distribution matching. *arXiv preprint arXiv:2503.06674*, 2025. 7, 10, 11

[44] Nanye Ma, Mark Goldstein, Michael S Albergo, Nicholas M Boffi, Eric Vanden-Eijnden, and Saining Xie. Sit: Exploring flow and diffusion-based generative models with scalable interpolant transformers. In *European Conference on Computer Vision*, pages 23–40. Springer, 2024. 9

[45] Yuhang Ma, Xiaoshi Wu, Keqiang Sun, and Hongsheng Li. Hpsv3: Towards wide-spectrum human preference score. In *Proceedings of the IEEE/CVF International Conference on Computer Vision*, pages 15086–15095, 2025. 2, 11

[46] Lars Mescheder, Andreas Geiger, and Sebastian Nowozin. Which training methods for gans do actually converge? In *International conference on machine learning*, pages 3481–3490. PMLR, 2018. 11

[47] Zichen Miao, Zhengyuan Yang, Kevin Lin, Ze Wang, Zicheng Liu, Lijuan Wang, and Qiang Qiu. Tuning timestep-distilled diffusion model using pairwise sample optimization. *arXiv preprint arXiv:2410.03190*, 2024. 2, 3, 7, 8, 9

[48] Maxime Oquab, Timothée Darcet, Théo Moutakanni, Huy V. Vo, Marc Szafraniec, Vasil Khalidov, Pierre Fernandez, Daniel Haziza, Francisco Massa, Alaaeldin El-Nouby, Mahmoud Assran, Nicolas Ballas, Wojciech Galuba, Russ Howes, Po-Yao (Bernie) Huang, Shang-Wen Li, Ishan Misra, Michael G. Rabbat, Vasu Sharma, Gabriel Synnaeve, Hu Xu, Hervé Jégou, Julien Mairal, Patrick Labatut, Armand Joulin, and Piotr Bojanowski. Dinov2: Learning robust visual features without supervision. *arXiv preprint arXiv:2304.07193*, 2023. 9

[49] William Peebles and Saining Xie. Scalable diffusion models with transformers. In *Proceedings of the IEEE/CVF international conference on computer vision*, pages 4195–4205, 2023. 2

[50] Dustin Podell, Zion English, Kyle Lacey, Andreas Blattmann, Tim Dockhorn, Jonas Müller, Joe Penna, and Robin Rombach. Sdxl: Improving latent diffusion models for high-resolution image synthesis. *arXiv preprint arXiv:2307.01952*, 2023. 2, 7

[51] Ben Poole, Ajay Jain, Jonathan T Barron, and Ben Mildenhall. Dreamfusion: Text-to-3d using 2d diffusion. *arXiv preprint arXiv:2209.14988*, 2022. 10

[52] Yuxi Ren, Xin Xia, Yanzuo Lu, Jiacheng Zhang, Jie Wu, Pan Xie, Xing Wang, and Xuefeng Xiao. Hyper-sd: Trajectory segmented consistency model for efficient image synthesis. *arXiv preprint arXiv:2404.13686*, 2024. 2, 3, 4, 5, 7, 8, 10, 11

[53] Kevin Roth, Aurelien Lucchi, Sebastian Nowozin, and Thomas Hofmann. Stabilizing training of generative adversarial networks through regularization. *Advances in neural information processing systems*, 30, 2017. 11

[54] Tim Salimans, Ian Goodfellow, Wojciech Zaremba, Vicki Cheung, Alec Radford, and Xi Chen. Improved techniques for training gans. *Advances in neural information processing systems*, 29, 2016. 11

[55] Tim Salimans, Ian Goodfellow, Wojciech Zaremba, Vicki Cheung, Alec Radford, and Xi Chen. Improved techniques for training gans. *Advances in neural information processing systems*, 29, 2016. 10

[56] Axel Sauer, Frederic Boesel, Tim Dockhorn, Andreas Blattmann, Patrick Esser, and Robin Rombach. Fast high-resolution image synthesis with latent adversarial diffusion distillation. In *SIGGRAPH Asia 2024 Conference Papers*, pages 1–11, 2024. 7, 8, 11

[57] Axel Sauer, Dominik Lorenz, Andreas Blattmann, and Robin Rombach. Adversarial diffusion distillation. In *European Conference on Computer Vision*, pages 87–103. Springer, 2024. 11

[58] Christoph Schuhmann, Romain Beaumont, Richard Vencu, Cade Gordon, Ross Wightman, Mehdi Cherti, Theo Coombes, Aarush Katta, Clayton Mullis, Mitchell Wortsman, et al. Laion-5b: An open large-scale dataset for training next generation image-text models. *Advances in neural information processing systems*, 35:25278–25294, 2022. 7, 9, 11

[59] John Schulman, Filip Wolski, Prafulla Dhariwal, Alec Radford, and Oleg Klimov. Proximal policy optimization algorithms. *arXiv preprint arXiv:1707.06347*, 2017. 4

[60] Team Seedream, Yunpeng Chen, Yu Gao, Lixue Gong, Meng Guo, Qiushan Guo, Zhiyao Guo, Xiaoxia Hou, Weilin Huang, Yixuan Huang, et al. Seedream 4.0: Toward next-generation multimodal image generation. *arXiv preprint arXiv:2509.20427*, 2025. 2

[61] Shitong Shao, Hongwei Yi, Hanzhong Guo, Tian Ye, Daquan Zhou, Michael Lingelbach, Zhiqiang Xu, and Zeke Xie. Magicdistillation: Weak-to-strong video distillation for large-scale few-step synthesis. *arXiv preprint arXiv:2503.13319*, 2025. 3

[62] Zhihong Shao, Peiyi Wang, Qihao Zhu, Runxin Xu, Junxiao Song, Xiao Bi, Haowei Zhang, Mingchuan Zhang, YK Li, Yang Wu, et al. Deepseekmath: Pushing the limits of mathematical reasoning in open language models. *arXiv preprint arXiv:2402.03300*, 2024. 11

[63] Xiangwei Shen, Zhimin Li, Zhantao Yang, Shiyi Zhang, Yingfang Zhang, Donghao Li, Chunyu Wang, Qinglin Lu, and Yansong Tang. Directly aligning the full diffusion trajectory with fine-grained human preference. *arXiv preprint arXiv:2509.06942*, 2025. 2, 5, 9, 10

[64] Jiaming Song, Chenlin Meng, and Stefano Ermon. Denoising diffusion implicit models. *arXiv preprint arXiv:2010.02502*, 2020. 2

[65] Yang Song, Jascha Sohl-Dickstein, Diederik P Kingma, Abhishek Kumar, Stefano Ermon, and Ben Poole. Score-based generative modeling through stochastic differential equations. *arXiv preprint arXiv:2011.13456*, 2020. 4, 10

[66] Z-Image Team. Z-image: An efficient image generation foundation model with single-stream diffusion transformer. *arXiv preprint arXiv:2511.22699*, 2025. 1, 2

[67] Bram Wallace, Meihua Dang, Rafael Rafailov, Linqi Zhou, Aaron Lou, Senthil Purushwalkam, Stefano Ermon, Caiming Xiong, Shafiq Joty, and Nikhil Naik. Diffusion model alignment using direct preference optimization. In *Proceedings of the IEEE/CVF Conference on Computer Vision and Pattern Recognition*, pages 8228–8238, 2024. 2, 3, 9, 10

[68] Yibin Wang, Yuhang Zang, Hao Li, Cheng Jin, and Jiaqi Wang. Unified reward model for multimodal understanding and generation. *arXiv preprint arXiv:2503.05236*, 2025. 11

[69] Yibin Wang, Yuhang Zang, Feng Han, Jiazi Bu, Yujie Zhou, Cheng Jin, and Jiaqi Wang. Unified personalized reward model for vision generation. *arXiv preprint arXiv:2602.02380*, 2026. 11

[70] Zhengyi Wang, Cheng Lu, Yikai Wang, Fan Bao, Chongxuan Li, Hang Su, and Jun Zhu. Prolificdreamer: High-fidelity and diverse text-to-3d generation with variational score distillation. *Advances in neural information processing systems*, 36:8406–8441, 2023. 10

[71] Haoning Wu, Zicheng Zhang, Weixia Zhang, Chaofeng Chen, Liang Liao, Chunyi Li, Yixuan Gao, Annan Wang, Erli Zhang, Wenxiu Sun, et al. Q-align: Teaching lmms for visual scoring via discrete text-defined levels. *arXiv preprint arXiv:2312.17090*, 2023. 11

[72] Jie Wu, Yu Gao, Zilyu Ye, Ming Li, Liang Li, Hanzhong Guo, Jie Liu, Zeyue Xue, Xiaoxia Hou, Wei Liu, et al. Rewarddance: Reward scaling in visual generation. *arXiv preprint arXiv:2509.08826*, 2025. 11

[73] Xiaoshi Wu, Yiming Hao, Keqiang Sun, Yixiong Chen, Feng Zhu, Rui Zhao, and Hongsheng Li. Human preference score v2: A solid benchmark for evaluating human preferences of text-to-image synthesis. *arXiv preprint arXiv:2306.09341*, 2023. 2, 3, 4, 7, 9, 11

[74] Xiaoshi Wu, Keqiang Sun, Feng Zhu, Rui Zhao, and Hongsheng Li. Human preference score: Better aligning text-to-image models with human preference. In *Proceedings of the IEEE/CVF International Conference on Computer Vision*, pages 2096–2105, 2023. 11

[75] Xiaoshi Wu, Yiming Hao, Manyuan Zhang, Keqiang Sun, Zhaoyang Huang, Guanglu Song, Yu Liu, and Hongsheng Li. Deep reward supervisions for tuning text-to-image diffusion models. In *European Conference on Computer Vision*, pages 108–124. Springer, 2024. 9

[76] Jiazheng Xu, Xiao Liu, Yuchen Wu, Yuxuan Tong, Qinkai Li, Ming Ding, Jie Tang, and Yuxiao Dong. Imagereward: Learning and evaluating human preferences for text-to-image generation. *Advances in Neural Information Processing Systems*, 36:15903–15935, 2023. 2, 3, 4, 5, 7, 9, 10, 11

[77] Jiazheng Xu, Yu Huang, Jiale Cheng, Yuanming Yang, Jiajun Xu, Yuan Wang, Wenbo Duan, Shen Yang, Qunlin Jin, Shurun Li, et al. Visionreward: Fine-grained multi-dimensional human preference learning for image and video generation. *arXiv preprint arXiv:2412.21059*, 2024. 11

[78] Yilun Xu, Weili Nie, and Arash Vahdat. One-step diffusion models with f-divergence distribution matching. *arXiv preprint arXiv:2502.15681*, 2025. 10

[79] Zeyue Xue, Jie Wu, Yu Gao, Fangyuan Kong, Lingting Zhu, Mengzhao Chen, Zhiheng Liu, Wei Liu, Qiushan Guo, Weilin Huang, et al. Dancegrpo: Unleashing grpo on visual generation. *arXiv preprint arXiv:2505.07818*, 2025. 2, 3, 9, 10

[80] Tianwei Yin, Michaël Gharbi, Taesung Park, Richard Zhang, Eli Shechtman, Fredo Durand, and Bill Freeman. Improved distribution matching distillation for fast image synthesis. *Advances in neural information processing systems*, 37:47455–47487, 2024. 2, 3, 7, 8, 9, 10

[81] Tianwei Yin, Michaël Gharbi, Richard Zhang, Eli Shechtman, Fredo Durand, William T Freeman, and Taesung Park. One-step diffusion with distribution matching distillation. In *Proceedings of the IEEE/CVF conference on computer vision and pattern recognition*, pages 6613–6623, 2024. 2, 10, 11

[82] Sihyun Yu, Sangkyung Kwak, Huiwon Jang, Jongheon Jeong, Jonathan Huang, Jinwoo Shin, and Saining Xie. Representation alignment for generation: Training diffusion transformers is easier than you think. In *International Conference on Learning Representations*, 2025. 9

[83] Aohan Zeng, Xin Lv, Zhenyu Hou, Zhengxiao Du, Qinkai Zheng, Bin Chen, Da Yin, Chendi Ge, Chengxing Xie, Cunxiang Wang, et al. Glm-5: from vibe coding to agentic engineering. *arXiv preprint arXiv:2602.15763*, 2026. 11

[84] Richard Zhang, Phillip Isola, Alexei A Efros, Eli Shechtman, and Oliver Wang. The unreasonable effectiveness of deep features as a perceptual metric. In *Proceedings of the IEEE conference on computer vision and pattern recognition*, pages 586–595, 2018. 10

[85] Yuxin Zhang, Weiming Dong, Fan Tang, Nisha Huang, Haibin Huang, Chongyang Ma, Tong-Yee Lee, Oliver Deussen, and Changsheng Xu. Prospect: Prompt spectrum for attribute-aware personalization of diffusion models. *ACM Transactions on Graphics (TOG)*, 42(6):1–14, 2023. 7

[86] Zhanjie Zhang, Quanwei Zhang, Huaizhong Lin, Wei Xing, Juncheng Mo, Shuaicheng Huang, Jinheng Xie, Guangyuan Li, Junsheng Luan, Lei Zhao, et al. Towards highly realistic artistic style transfer via stable diffusion with step-aware and layer-aware prompt. *arXiv preprint arXiv:2404.11474*, 2024. 7

[87] Kaiwen Zheng, Huayu Chen, Haotian Ye, Haoxiang Wang, Qinsheng Zhang, Kai Jiang, Hang Su, Stefano Ermon, Jun Zhu, and Ming-Yu Liu. Diffusionnft: Online diffusion reinforcement with forward process. *arXiv preprint arXiv:2509.16117*, 2025. 2, 3, 10

[88] Kaiwen Zheng, Yuji Wang, Qianli Ma, Huayu Chen, Jintao Zhang, Yogesh Balaji, Jianfei Chen, Ming-Yu Liu, Jun Zhu, and Qinsheng Zhang. Large scale diffusion distillation via score-regularized continuous-time consistency. *arXiv preprint arXiv:2510.08431*, 2025. 10, 11

[89] Daniel M Ziegler, Nisan Stiennon, Jeffrey Wu, Tom B Brown, Alec Radford, Dario Amodei, Paul Christiano, and Geoffrey Irving. Fine-tuning language models from human preferences. *arXiv preprint arXiv:1909.08593*, 2019. 3, 4